ACS Catalysis

Letter

pubs.acs.org/acscatalysis

Monomolecular Skeletal Isomerization of 1-Butene over Selective Zeolite Catalysts

Donghui Jo,[†] Suk Bong Hong,*[,†] and Miguel A. Camblor*[,‡]

[†]Center for Ordered Nanoporous Materials Synthesis, School of Environmental Science and Engineering, POSTECH, Pohang 790-784, Korea

[‡]Instituto de Ciencia de Materiales de Madrid (ICMM), Consejo Superior de Investigaciones Cientificas (CSIC), Sor Juana Inés de la Cruz 3, 28049 Madrid, Spain

Supporting Information

ABSTRACT: The mechanism of the 1-butene skeletal isomerization catalyzed by zeolites has remained elusive. We present direct evidence that even the initial isobutene formation over H-ferrierite, the best-known isomerization catalyst, is monomolecular in nature, whereas a bimolecular pathway is significant over the unselective H-ZSM-5. We also report that medium-pore high-silica H-HPM-1 outperforms H-ferrierite in selectively forming isobutene. This new catalyst displays a high activity and selectivity from the onset of the reaction, as well as an excellent resistance to deactivation, thanks to its anomalously weak acidity and low acid site density, together with an ability to effectively isolate reactant molecules from one another.

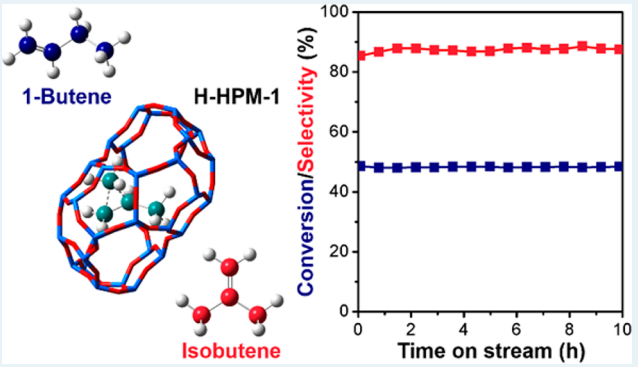

KEYWORDS: *1-butene skeletal isomerization, molecular dynamics, monomolecular pathway, zeolites, ^{13}C scrambling*

Butene isomers (C_4H_8: 1-butene, *cis*- and *trans*-2-butenes, and 2-methylpropene, also known as isobutene) are mainly produced as byproducts in various petrochemical processes such as the catalytic cracking of petroleum fractions, ethylene oligomerization, and methanol-to-olefin process.[1] Among them, isobutene has led the demand over the last few decades, mainly because of its use to make methyl *tert*-butyl ether (MTBE, which is currently being phased out as a gasoline additive in several states in the U.S.), butyl rubber, and many chemical intermediates (including methacrolein, neohexene, pivalic acid, etc.).[2] The petrochemical industry has been making use of catalytic skeletal isomerization reactions that allow tuning the production to the most desired product. Up to now, a wide variety of microporous solid acids with medium pores, particularly the zeolite ferrierite (zeolite framework type FER) in its proton form (H-FER), have been in extensive industrial use and under intensive academic investigation.[3]

The performance of H-FER, known as the best catalyst for this reaction thus far, is intriguing because it varies with time on stream (TOS): a high selectivity is observed only over the deactivated catalyst with carbonaceous deposits present. Consequently, the yield to the desired isobutene goes through a maximum and then declines. Here we report that H-HPM-1, a new high-silica zeolite with the STW framework type,[4] displays an essentially constant activity and selectivity, producing a high and constant yield of isobutene. Furthermore, H-HPM-1 is deactivated much more slowly than H-FER. This new zeolite contains a three-dimensional (3D) chiral framework of $P6_122$ or $P6_522$ space group containing helical 10-ring pores (5.8 × 5.4 Å) intersected by straight 8-ring pores (4.5 × 3.2 Å), as shown in Figure 1.[4b] We also provide clear experimental evidence that the selective isobutene formation over both H-FER (including the fresh catalyst) and H-HPM-1 is dominated by a "true" monomolecular pathway which does not require strong acidity. By contrast, there is significant

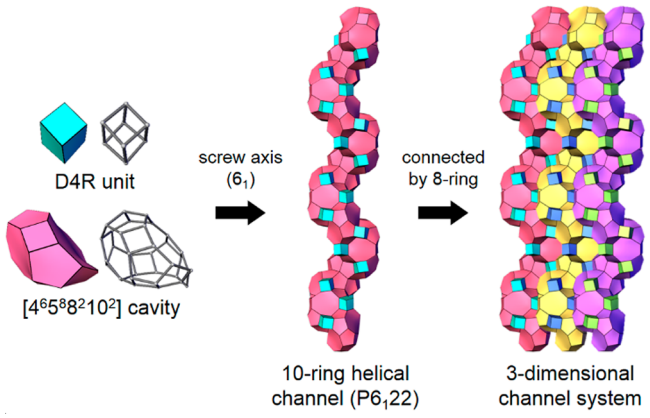

Figure 1. Tiling presentation of STW structure.

Received: January 30, 2015
Revised: March 7, 2015
Published: March 9, 2015

DOI: 10.1021/acscatal.5b00195
ACS Catal. 2015, 5, 2270−2274

contribution of a bimolecular pathway over the unselective H-ZSM-5 catalyst. To date, the prevailing mechanism for the isobutene formation over H-FER is still far from well understood, being subject to vigorous debate.

Figure 2a–c shows 1-butene conversion and isobutene selectivity and yield as a function of TOS in the skeletal

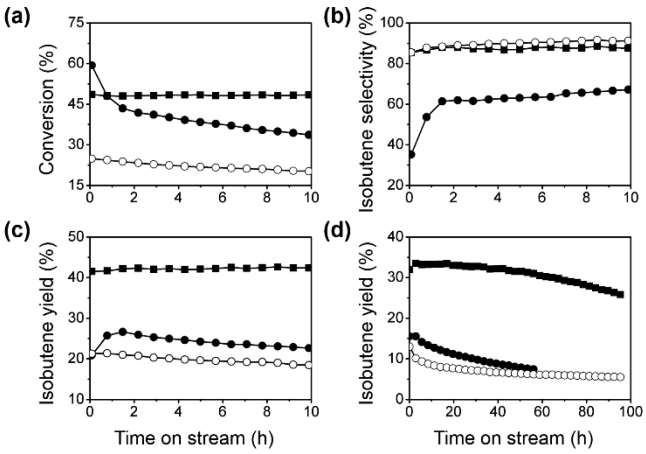

Figure 2. (a) 1-Butene conversion and (b) selectivity to and (c) yield in isobutene at 673 K and 7.5 h^{-1} WHSV and (d) yield in isobutene at 673 K and 24.0 h^{-1} WHSV in the 1-butene skeletal isomerization over zeolites: H-HPM-1(110), ■; H-FER(85), ○; H-FER(8.9), ●. The values in parentheses of the catalyst identification are Si/Al ratios.

isomerization of 1-butene over H-FER with Si/Al = 8.9 (obtained from Tosoh) and 85 (synthesized in the lab) and H-HPM-1 (Si/Al = 110) measured at 673 K and 7.5 h^{-1} weight hourly space velocity (WHSV). Undoubtedly, H-HPM-1 is characterized by a high 1-butene conversion and a high isobutene selectivity over the period of TOS studied, including the very onset of the reaction, also observed at lower reaction temperatures (e.g., 623 K; Figure S1). Consequently, it produces a steadily high yield of isobutene. Moreover, H-HPM-1 displays higher resistance to deactivation than H-FER, even when the space velocity is more than tripled (Figure 2d). The stability and selectivity of H-FER during 1-butene skeletal isomerization are known to increase as its Al content decreases, while its activity decreases.[55] As seen in Figure 2, when the Si/Al ratio of the commercial catalyst is increased to values close to those in H-HPM-1, the resulting H-FER(85) shows a quite high selectivity but a poor activity, thus producing a meager isobutene yield.

H-HPM-1 and H-FER(85) contain tetrahedral $Al(OSi)_4$ units with negligible amounts of extraframework Al species (see ^{27}Al MAS NMR spectra Figure 3a) and a large surface area (550 and 370 m^2 g^{-1} respectively, Figure S2). Their acid site density, determined by ammonia temperature-programmed desorption (TPD), is around a tenth of that in H-FER(8.9) (Figure 3b), in good agreement with their respective Si/Al ratios (110 and 85 vs 8.9). Unexpectedly, however, the acid sites in H-HPM-1 are of medium to weak strength, although H-FER(85), with a similar density of sites, presents stronger acid sites, as revealed by the large drift of the TPD profile to the high temperature side (the profile of H-FER(8.9) is drifted by a much larger amount, likely caused by readsorption and constrained diffusion due to its much larger acid site density).[6a] Given the catalytic results in Figure 2, therefore, it is clear that

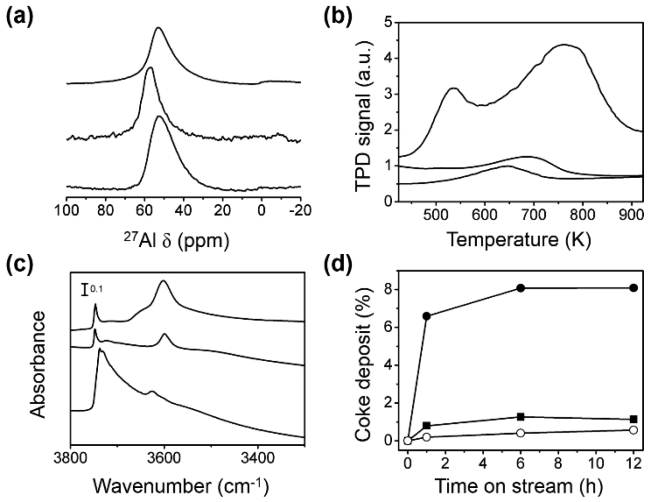

Figure 3. (a) ^{27}Al MAS NMR spectra; (b) ammonia TPD curves; (c) IR spectra in the OH stretching region of (from bottom to top) H-HPM-1, H-FER(85), and H-FER(8.9); and (d) their coke amounts (H-HPM-1, ■; H-FER(85), ○; H-FER(8.9), ●) formed during 1-butene skeletal isomerization at 673 K and 7.5 h^{-1} WHSV for different times.

zeolite acidity does not need to be strong in order to selectively produce isobutene.

In general, the lower Al content a zeolite has, the lower density of acid sites it possesses, whereas the acid strength tends to increase until ca. Si/Al ratio of 10 due to the increased average electronegativity of the framework with a higher Si/Al ratio.[6] Thus, very high-silica zeolites usually display strong acid sites, although the acid strength is also structure-dependent.[6a] The medium/weak acidity of high-silica H-HPM-1 must be thus due to the local structure around the acid sites. The ^{29}Si MAS NMR spectrum of H-HPM-1 shows three well-resolved resonances due to $Si(OSi)_3OAl$ (−102.2 ppm) and to two $Si(OSi)_4$ species (−109.5 and −115.8 ppm) corresponding to the Si atoms in and out, respectively, of double-4-ring (D4R) units (structural units containing 8 Si roughly at the vertices of a cube bonded through O bridges along the cube edges). Deconvolution of the spectrum affords to calculate an Si/Al ratio of 107 (Figure S3), in excellent agreement with the expected value (110).

Although there is no consensus on the possible correlation between the local structure around Al and the acid strength of the bridging Al-(OH)-Si group,[7] we deem likely that the sitting of Al in D4Rs, which have characteristically small T-O-T angles and are rare for very high-silica zeolites, is responsible for the unusually weak acidity of H-HPM-1. In fact, the ^{27}Al MAS NMR and ammonia TPD data (Figures S4 and S5) of H-ITQ-12 (ITW) with Si/Al = 96, another high-silica zeolite containing a high density of D4Rs, also reveal medium to low acid strength, supporting our conclusion. This can be further established by IR spectroscopy. H-FER(8.9) shows an intense, broad band around 3600 cm^{-1} in the OH stretching region, evidencing the high density and strong nature of its acid sites, whereas H-FER(85) shows a small peak at identical position. However, H-HPM-1 exhibits a much weaker band at 3622 cm^{-1} (Figure 3c), indicative of a stronger O–H bond and, hence, a lower acid strength.[8] H-ITQ-12 gives two bands around 3622 and 3573 cm^{-1}, revealing the existence of two types of acid sites assignable to weak and strong sites due to Al in and out of D4R units, respectively (Figure S5). The lack of

DOI: 10.1021/acscatal.5b00195
ACS Catal. 2015, 5, 2270–2274

the latter band in H-HPM-1 suggests that, unlike the case of H-ITQ-12, Al is preferentially located at D4Rs in H-HPM-1. The higher resistance to coke formation on zeolites with higher Si/Al ratios (Figures 3d) may be due to their low acid site density, rather than to their acid strength.

There are at least three possible mechanisms for the acid-catalyzed isomerization of 1-butenes to isobutene:[3b,c] monomolecular, bimolecular, and pseudomonomolecular. The true monomolecular mechanism is based on the formation of a protonated cyclopropene moiety that may be broken to give a secondary carbenium ion (that produces a 1-butene molecule by losing H^+) or a primary carbenium ion, which will be able to rearrange to give isobutene. This mechanism is fundamentally selective to isobutene, because when the primary cation does not yield isobutene, it gives back *n*-butenes. However, the monomolecular pathway is generally considered not favored due to the formation of an unstable primary carbenium ion. The bimolecular mechanism, which requires strong acid sites, consists of a dimerization followed by cracking and is unselective, always yielding a fraction of propene and pentenes (and even hexenes and heptenes), in addition to *n*-butenes. Finally, in the pseudomonomolecular pathway, the active site is proposed to be a tertiary carbenium ion trapped close to the pore mouth in a coke-like environment. This cation would react with 1-butene, producing a secondary carbenium ion that can rearrange to a more stable tertiary carbenium ion which, after desorption, would produce isobutene. Although significant controversy still exists, the performance of, for instance, H-FER has been explained as follows: initially, the most favorable but unselective bimolecular reaction would take place with high activity. As coke is formed by side-reactions and pores start getting blocked, the formation of tertiary carbenium species in the pore mouth would be able to catalyze the selective formation of isobutene. This pore mouth catalysis would explain the very high activity of H-FER nanoneedles and of micro/mesoporous H-FER zeolite.[9]

This explanation, however, does not hold for H-HPM-1: high degrees of its 1-butene reactivity and isobutene selectivity from the onset of the reaction require a different explanation, further supported by the behavior at a higher WHSV (Figure 2d). Additionally, H-HPM-1 is made of heavily interpenetrated submicrometer crystals (Figure S6), so its exceptional isobutene yield cannot be due to any pore mouth effect enhanced in a nanocrystalline catalyst, which is corroborated by its small external surface (70 $m^2\ g^{-1}$).

Gas chromatography−mass spectroscopy (GC-MS) analyses of the products obtained using ^{13}C-labeled 1-butene (i.e., 1-[1-^{13}C]butene) as a reactant in 1-butene skeletal isomerization have long been recognized as a reliable method to check whether the bimolecular pathway operates predominantly.[10] If isobutene is formed from 1-[1-^{13}C]butene via the monomolecular or pseudomonomolecular pathway, the ^{13}C atom could not migrate to a different molecule, and thus, the isobutene produced should possess only one ^{13}C atom. In the bimolecular reaction, however, the octyl carbenium ion isomers containing two ^{13}C atoms, produced by dimerization, would continue to isomerize among them.[5b] Because the two ^{13}C atoms should thus spread out randomly in these carbenium ions during the reaction, the isobutene molecules produced via a bimolecular pathway may contain zero, one, or two ^{13}C atoms. This can be eventually evidenced in the mass spectrum of isobutene by the intensity increase of the fragments one mass atomic unit smaller (M-1) or larger (M+1) than the molecular ion (M), the so-called ^{13}C scrambling. Extensive ^{13}C scrambling has been repeatedly reported during 1-butene skeletal isomerization over fresh H-FER, but not over the aged catalyst.[10] However, in those reports, scrambling data on fresh H-FER were obtained under static conditions (batch reaction), in which bimolecular rereaction between products can occur in the absence of a continuous supply of reactant molecules. To avoid this, we carried out the ^{13}C scrambling experiments over H-FER(8.9) and H-HPM-1 in a flow reactor under the same dynamic conditions as those (673 K and 7.5 h^{-1} WHSV) used to obtain the catalytic results in Figure 2a−c. In contrast to the results previously reported, ^{13}C scrambling in isobutene, as well as in the other three butene isomers, is not largely significant in fresh H-FER(8.9). Additionally, it is hardly perceptible in fresh H-HPM-1, aged H-FER, and aged H-HPM-1 (Figures 4 and S7). However, the mass spectra of all pentene byproducts are characterized by extensive ^{13}C scrambling (Figures 4 and S8), as expected from their necessary formation by the bimolecular pathway. We also note that the distribution of pentene isomers is essentially identical to the thermodynamic distribution,[11] suggesting that cracking of dimers over these two medium-pore zeolites is not shape-selective.

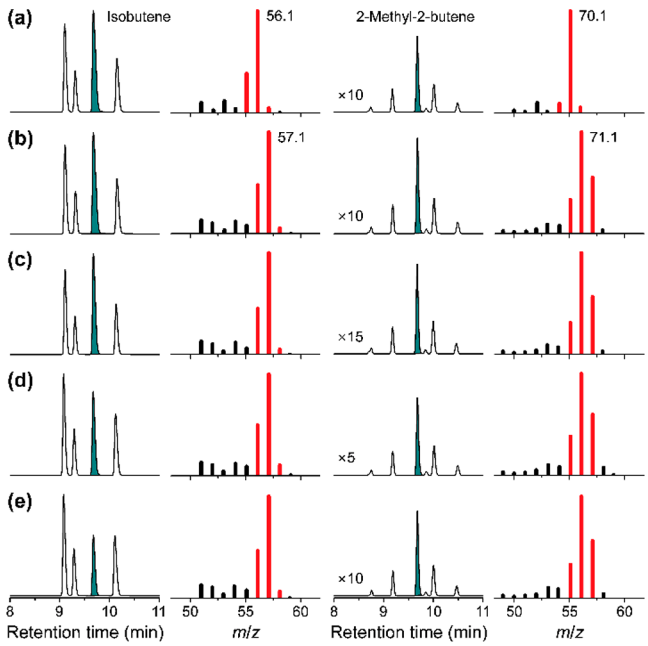

Figure 4. Online GC-MS analyses of isobutene and 2-methyl-2-butene produced after 1-butene skeletal isomerization using unlabeled 1-butene over (a) fresh H-HPM-1 and using 1-[1-^{13}C]butene over (b) fresh H-HPM-1, (c) aged H-HPM-1, (d) fresh H-FER(8.9), and (e) aged H-FER(8.9) at 673 K and 7.5 h^{-1} WHSV for 5 min. The isobutene and 2-methyl-2-butene peaks in gas chromatograms are marked in dark cyan, and the M-1, M, and M+1 peaks in mass spectra are marked in red for the clear observation of ^{13}C scrambling.

Therefore, both mono- and bimolecular reactions, which are the main sources of isobutene and pentenes, respectively, occur from the onset of the reaction over H-FER(8.9), as well as over H-HPM-1, despite notable differences in their catalytic performance. The bimolecular path has a much larger contribution over fresh H-FER(8.9) than over fresh HPM-1, but this contribution is gradually reduced with time, leading to large changes in the performance of the former zeolite over time. Thus, the prevailing mechanism for the selective

DOI: 10.1021/acscatal.5b00195
ACS Catal. 2015, 5, 2270−2274

isobutene formation over both catalysts is monomolecular in nature. The GC-MS results in Figure 4 also show that the rapid decrease in conversion and increase in isobutene selectivity over H-FER(8.9) with TOS is mainly due to changes in the relative contribution of both reaction pathways, with the bimolecular reaction being disfavored as the zeolite ages.

We additionally carried out ^{13}C scrambling experiments (Figure S9 and S10) over fresh H-FER(85) and H-ZSM-5 with Si/Al = 95 (Tosoh), which is a well-known nonselective catalyst for the 1-butene isomerization (Figure S11). As expected, the mass spectrum of isobutene in H-ZSM-5 shows extensive ^{13}C scrambling, supporting that a bimolecular path contributes significantly to the formation of isobutene over fresh H-ZSM-5, in contrast with H-FER(85). Although the strength and density of acid sites and deactivation behavior are similar for H-ZSM-5 and H-FER(85), the former is much less selective to isobutene (Figure S5). It appears that the density rather than the strength of acid sites is mostly responsible for deactivation through oligomerization beyond dimerization, whereas there has to be a large influence of the zeolite structure or pore architecture on the activity and selectivity of the reaction.

In terms of pore shape, a more elliptical pore leads to a higher isobutene selectivity but simultaneously a lower conversion, so H-FER with a suitable degree of ellipticity (0.629) displays a remarkable performance in the 1-butene skeletal isomerization by pore mouth catalysis.[3d] However, H-HPM-1 with quite a low ellipticity of 0.386, similar to that of H-ZSM-5 (0.374 and 0.323; sinusoidal and straight channels, respectively.), shows simultaneously high conversion just below the H-ZSM-5 level and high selectivity at the H-FER level. When compared to H-FER(8.9) and H-FER(85), we conclude that the weak zeolite acidity and low acid site density disfavors a bimolecular mechanism, thus increasing isobutene selectivity. Because H-ZSM-5 with Si/Al = 95 shows very nonselective behavior, however, the high selectivity of H-HPM-1 cannot be explained only by the low acid site density.

To further understand the unique selectivity of H-HPM-1, molecular mechanics and molecular dynamics simulations about STW and MFI zeolites with less elliptical 10-ring pore shapes, were carried out using the Sorption and Forcite modules in Materials Studio 7.0, respectively.[12] The CVFF force field and periodic boundary conditions were applied in all the calculations.[13] When we performed the Grand Canonical Monte Carlo (GCMC) simulations using Sorption module of 1-butene at 673 K in STW and MFI (Figure S12), these two zeolites were calculated to have equilibrium loadings at a constant fugacity of 101.33 kPa of 3.9 and 6.6 molecules per unit cell (60 T atoms for STW and 96 T atoms for MFI), respectively.

These results suggest a reactant isolation effect on the catalytic behavior of H-HPM-1. Because its channels are a succession of cavities and there are six cavities per unit cell, the calculated loading will disfavor close contacts and hence a bimolecular path in this zeolite. On the other hand, the simulated annealing calculations using Forcite module in the NVE ensemble of the equilibrium position of 1-butene in STW and MFI reveal large separations between molecules in the former and rather close contacts in the latter (Figure 5). Channel intersections in MFI can provide suitable space for dimerization, unlike the cavity-based STW channels. We think that the unique pore structure of STW may be efficient for isolating 1-butene reactant molecules from one another during the reaction, facilitating a true monomolecular reaction mechanism, despite the circular shape of its 10-ring pores.

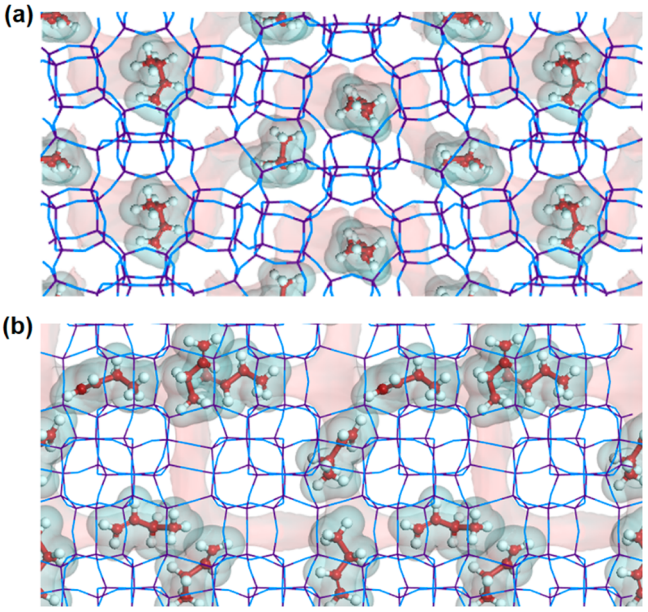

Figure 5. Equilibrium positions of 1-butene molecules within (a) STW (4 molecules per unit cell with 60 Si atoms) and (b) MFI (7 molecules per unit cell with 96 Si atoms) structures determined using simulated annealing. Red and white balls and purple and blue lines indicate C, H, Si, and O atoms, respectively. The regions marked in light blue and light brown represent the van der Waals surface of 1-butene and the accessible solvent surface.

In summary, we have demonstrated that the selective isobutene formation over H-FER and H-HPM-1 proceeds by a true monomolecular mechanism. The exceptional performance of H-HPM-1 arises from a combination of factors: (1) low acid site density and reactant isolation effect, both disfavoring oligomerization reactions; (2) low acid strength, disfavoring cracking; and (3) low 10-ring pore ellipticity, which favors a high activity by disfavoring pore mouth catalysis. All that originate from the unique structure of this new zeolite which consists mainly of D4Rs and contains a 3D 10-ring circular pore system made of a string of cavities.

■ ASSOCIATED CONTENT

Supporting Information

The following file is available free of charge on the ACS Publications website at DOI: 10.1021/acscatal.5b00195.

Experimental section, computational details, characterization data, and additional results (PDF)

■ AUTHOR INFORMATION

Corresponding Authors

*E-mail: sbhong@postech.ac.kr.

*E-mail: macamblor@icmm.csic.es.

Notes

The authors declare no competing financial interest.

The authors have applied for a patent based on the reaction reported in this paper.

■ ACKNOWLEDGMENTS

This work was supported by the NCRI (2012R1A3A-2048833) and BK 21-plus programs through the National Research

DOI: 10.1021/acscatal.5b00195
ACS Catal. 2015, 5, 2270−2274

Foundation of Korea and by the Spanish Ministry of Economy and Competitiveness (MAT2012-31759). We thank S. H. Cha, K. H. Lee, and A. Rojas for technical assistance.

REFERENCES

(1) Tanabe, K.; Hölderich, W. F. *Appl. Catal., A* **1999**, *181*, 399−434.
(2) (a) Haworth, J. P.; Baldwin, F. P. *Ind. Eng. Chem.* **1942**, *34*, 1301−1308. (b) Moens, L.; Puiz, P.; Delmon, B.; Devillers, M. *Appl. Catal., A* **1999**, *180*, 299−315. (c) Mol, J. C. *J. Mol. Catal. A: Chem.* **2004**, *213*, 39−45. (d) Brilman, D. W. F.; van Swaaij, W. P. M.; Versteeg, G. F. *Chem. Eng. Sci.* **1999**, *54*, 4801−4809. (e) Deeba, M.; Ford, M. E. *J. Org. Chem.* **1998**, *53*, 4594−4596.
(3) (a) Meriaudeau, P.; Naccache, C. *Adv. Catal.* **1999**, *44*, 505−543. (b) van Donk, S.; Bitter, J. H.; de Jong, K. P. *Appl. Catal., A* **2001**, *212*, 97−116. (c) Guisnet, M.; Andy, P.; Gnep, N. S.; Travers, C.; Benazzi, E. *J. Chem. Soc., Chem. Commun.* **1995**, 1685−1686. (d) Lee, S.-H.; Shin, C.-H.; Hong, S. B. *J. Catal.* **2004**, *223*, 200−211. (e) Seo, G. *Catal. Surv. Asia* **2005**, *9*, 139−146.
(4) (a) Rojas, A.; Arteaga, O.; Kahr, B.; Camblor, M. A. *J. Am. Chem. Soc.* **2013**, *135*, 11975−11984. (b) Rojas, A.; Camblor, M. A. *Angew. Chem., Int. Ed.* **2012**, *51*, 3854−3856.
(5) (a) Asensi, M. A.; Martínez, A. *Appl. Catal., A* **1999**, *183*, 155−165. (b) Rutenbeck, D.; Papp, H.; Ernst, H.; Schwieger, W. *Appl. Catal., A* **2001**, *208*, 153−161. (c) Yang, B.; Jiang, J.-G.; Xu, H.; Liu, Y.; Peng, H.; Wu, P. *Appl. Catal., A* **2013**, *455*, 107−113.
(6) (a) Niwa, M.; Katada, N. *Catal. Surv. Jpn.* **1997**, *1*, 215−226. (b) Jacobs, P. A.; Mortier, W. J.; Uytterhoeven, J. B. *J. Inorg. Nucl. Chem.* **1978**, *40*, 1919−1923.
(7) (a) Rabo, J. A.; Gajda, G. J. *Catal. Rev.: Sci. Eng.* **1989**, *31*, 385−430. (b) Schröder, K.-P.; Sauer, J.; Leslie, M.; Catlow, C. R. A.; Thomas, J. M. *Chem. Phys. Lett.* **1992**, *188*, 320−325. (c) Eichler, U.; Brändle, M.; Sauer, J. *J. Phys. Chem. B* **1997**, *101*, 10035−10050. (d) Katada, N.; Suzuki, K.; Noda, T.; Sastre, G.; Niwa, M. *J. Phys. Chem. C* **2009**, *113*, 19208−19217.
(8) Chu, C. T.-W.; Chang, C. D. *J. Phys. Chem.* **1985**, *89*, 1569−1571.
(9) (a) Lee, Y.; Park, M. B.; Kim, P. S.; Vicente, A.; Fernandez, C.; Nam, I.-S.; Hong, S. B. *ACS Catal.* **2013**, *3*, 617−621. (b) Khitev, Y. P.; Ivanova, I. I.; Kolyagin, Y. G.; Ponomareva, O. A. *Appl. Catal., A* **2012**, *441*−*442*, 124−135.
(10) (a) Meriaudeau, P.; Bacaud, R.; Hung, L. H.; Vu, A. T. *J. Mol. Catal. A: Chem.* **1996**, *110*, L177−L179. (b) de Jong, K. P.; Mooiweer, H. H.; Buglass, J. G.; Maarsen, P. K. *Stud. Surf. Sci. Catal.* **1997**, *111*, 127−138.
(11) Mäurer, T.; Kraushaar-Czarnetzki, B. *J. Catal.* **1999**, *187*, 202−208.
(12) *Materials Studio 7.0*; Accelrys Inc.: San Diego, CA, 2013.
(13) Dauber-Osguthorpe, P.; Roberts, V. A.; Osguthorpe, D. J.; Wolff, J.; Genest, M.; Hagler, A. T. *Proteins: Struct., Funct., Genet.* **1988**, *4*, 31−47.

DOI: 10.1021/acscatal.5b00195
ACS Catal. 2015, 5, 2270−2274